

# Prediction of Tidal Current Using FVCOM Hydrodynamic Model in Khuran Strait of Persian Gulf

Hassan Kazemi<sup>1</sup>, Abbas Abedini<sup>1\*</sup>, Bahman Tajfirooz<sup>2</sup>

<sup>1\*</sup> School of Surveying and Geospatial Engineering, College of Engineering, University of Tehran, Tehran, Iran; [aabedeni@ut.ac.ir](mailto:aabedeni@ut.ac.ir), [hassankazemi@ut.ac.ir](mailto:hassankazemi@ut.ac.ir)

<sup>2</sup> Darya Tarsim Consulting Engineer Co., Tehran, Iran; [bahman.tajfirooz@gmail.com](mailto:bahman.tajfirooz@gmail.com)

## ARTICLE INFO

### Article History:

Received: 5 Feb 2024

Accepted: 16 Oct 2024

### Keywords:

FVCOM model

Hydrodynamic

Tidal current

Current direction

Current speed

## ABSTRACT

In recent years, the study of tidal currents has gained special importance due to economic, political, and environmental considerations, as well as its implications for maritime transport, navigational safety, and offshore structures. The Khuran Strait, located near the Strait of Hormuz in the Persian Gulf, is one of the most significant maritime areas. Thus, understanding tides, tidal currents, and their predictions is crucial in this region. We utilized the FVCOM model to simulate the speed and direction of tidal currents in the channel. The model's main inputs include the roughness coefficient, salinity, temperature, density, bathymetric data, and tidal information. Additionally, tidal time series were applied to the model using eight harmonic components. To evaluate the hydrodynamic model, we compared simulated current speeds and directions, as well as water levels, with observed data from specific locations. The results indicated a correlation of 75% for speed values and 89% for current direction. The RMSE values were 0.09 m/s for speed and 0.35 degrees for current direction. We used parameters such as RMSE and RV for statistical evaluation. Using the results of the FVCOM model, a Tidal Current Diamond prediction was presented.

## 1. Introduction

Ocean currents have always been significant for countries, particularly those near coastal areas or located in semi-closed basins. Most oil and gas resources, along with resource exploration, navigation, and power and communication transmission lines between the sea and coastal regions, are influenced by these currents. Additionally, ocean currents impact the geography of coastal areas. In the southern waters of Iran, there are thousands of aquatic species. Due to environmental factors, the presence of transmission and communication lines, as well as tourist resort projects, utilizing these vast resources necessitates the design of structures and infrastructure that can withstand these currents. The presence of major ports such as Shahid Bahonar, Shahid Rajae, and the Persian Gulf Shipyard Complex, along with Qeshm Island, Laft, and Khamir ports, contributes to the channel's importance for hydrodynamic studies. The area features a significant tidal range, with tides measuring approximately 3 meters on the northern coast of Qeshm Island and about 4.5 meters in other areas. Given the strategic and geographical conditions of this

channel, it is recognized as a critical region for our country. Ocean currents are driven by various factors, including tidal forces, the gravitational pull of the moon and sun, wind, temperature differences, and thermohaline circulation [1]. This channel is located between the northern shore of Qeshm Island and the southern coasts, in Khuran Strait between 26°44' to 26°58'N latitude and 31°55' to 55°48'E longitude (As has been shown study area in Figure 1).

On the northern, eastern and southern boundaries of the area are located respectively: Pohl, Pir jazireh, Upper and Lower Tashtagan, the city of Khamir, & old Laft, the port of Laft, Gawarzin & Khuran, Soheili, Tabl, Dorbani and Guran. Mangrove forest was first protected under the name of Mangrove Protected Area in 1972 with an area of 82360 hectares, then by increasing its area to 85686 hectares in 1975, considered as National Park. This area is now protected as Mangrove Protected Area under the management of the General Environment Department of Hormozgan Province.

Based on information obtained from three synoptic stations in Bandar-e Abbas, Bandar-e Lengeh, and Qeshm Island, the studied area exhibits a dry climate

according to De Martonne's climate classification, with an average annual temperature ranging from 25 to 27 degrees Celsius. Geologically, this area is part of the folded Zagros mountain range and has been tectonically influenced by the Arabian Plate throughout geological periods [2].

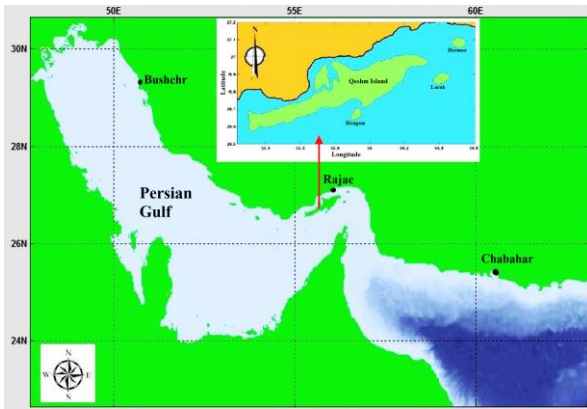


**Figure 1. The location of Khuran channel in Persian Gulf**

Several studies have focused on hydrodynamic modeling and the simulation of ocean water movement. Notable contributions include Chen, Liu [3], who developed an unstructured grid finite volume three-dimensional ocean model to study oceanic and coastal flows. Building on this, Wu and Tang [4] expanded high-resolution coastal ocean modeling (FVCOM) for Dartmouth Port, near Apponagansett Bay and Clarks Cove. Their series of experiments compared different modeling approaches to evaluate the impacts of sea level rise due to weather conditions, flow patterns, and wave distributions. These evaluations considered various dynamic forces, including wind direction and wave-current interactions. The results indicated that over a period of one hundred years, under easterly storm conditions, the rise in sea level caused by weather could significantly increase the potential flood areas by approximately 60% for each foot of sea level rise [3]. Cowles [5] significantly reduced the running time of the FVCOM model for the Gulf of Maine through parallel processing, leading to lower costs compared to previous years.

Wu and Tang [4] aimed to achieve accurate simulations of small-scale coastal ocean phenomena by integrating a computational fluid dynamics (CFD) model with the finite-volume coastal ocean model (FVCOM).

In the FVCOM model, current values are discretized using a triangulated grid for the horizontal planes and a separate grid for the vertical direction.

Using this method and convection equations, the horizontal speed in the vertical direction is determined, along with the water surface height and average values, which are directly influenced by the horizontal speeds. This process does not affect external forces. Additionally, these grids can

optionally overlap, providing optimal flexibility in coupling different models.

To facilitate the coupling of the two models, we need grid nodes at the interface and utilize fixed elements, or intermediate nodes, within the FVCOM grid [4].

Sabatino and Thurlbeck [6] studied the modeling of sea surface waves in Clyde Bay, located in the southwest of Scotland. Water level fluctuations due to tsunami disturbances arising from changes in the climate system (such as very low or high pressure) can result in alterations in water levels. Positive changes can cause flooding, damaging coastal infrastructure and leading to casualties. To mitigate flood damage, they designed a warning system by developing a hydrodynamic model. They simulated water circulation in the Firth of Clyde and the North Channel using the FVCOM model developed by Chen, Liu [3] to simulate flow in estuary areas. Li and Chen [7] studied two major storm systems for flood risk in Massachusetts coast: tropical cyclones and catastrophic tropical cyclones. Coastal flooding occurs when wind-driven waves combine with high tides during storms. They established a northeast coastal ocean forecast system (NECOFS). By applying the FVCOM model to NECOFS, they investigated the impact of rising water levels due to climate change on coastal flooding caused by future hurricanes along the Massachusetts coast. This was evaluated by testing the model to forecast flooding in Boston Harbor and South End coastal areas under different sea level rise (SLR) scenarios over a century or under easterly storm conditions. The results indicated that with rising sea levels, the stability of the northeast coast of the United States will be highly vulnerable to hurricanes driven by wind. This finding is consistent with the observed increase in the intensity of surface waves caused by hurricanes over the last decade. The model also demonstrated that the responses of waves and surface currents to rising sea levels were completely non-linear. The effects of rising sea levels on coastal flooding caused by future hurricanes should be investigated using models that include wave-current interactions. Xu, Canals [8] studied Puerto Rico and the US Virgin Islands (PRVI) using the finite-volume community ocean model (FVCOM). Unlike traditional ocean models based on a grid, FVCOM is composed of staggered prismatic cells with triangular elements on the horizontal plane, providing a more accurate geometric representation of complex coastlines. Modeled sea surface temperature results were confirmed by observational data, showing a clear decrease in the Root Mean Square Error (RMSE). Statistical comparisons with Acoustic Doppler Current Profiler (ADCP) observations and moored current meters indicated significant improvements in ocean current modeling compared to the AMSEAS model, particularly at higher frequencies under strong tidal conditions, where the FVCOM model exhibited superior bathymetric resolution. Bairamzadeh, Siadat

Mousavi [9] employed the FVCOM model for hydrodynamic modeling of the Persian Gulf and the Sea of Oman to simulate current patterns for the first six months of 2013, demonstrating the model's effectiveness in these regions. Razzaghi, Haghshenas [10] designed a current forecast system for the Persian Gulf, and comparisons between flow simulation results and observational data further confirmed the model's success in simulating flow dynamics. Sadrinasab, Einali [11] studied the Arvandrud River plume, the primary source of fresh water entering the Persian Gulf, which holds significant military and environmental importance.

Shariatmadari, Siadat-Mousavi [12] studied renewable energy sources, primarily derived from solar energy, in response to the increasing reliance on non-renewable fuels and their detrimental effects on the survival of numerous species. Sohrabi Athar, Ardalan [13] aimed to develop a two-dimensional hydrodynamic tidal model for the Persian Gulf (PG2017) using 2D-MIKE21 software. They analyzed instantaneous changes in water levels while accounting for variations in the seabed friction coefficient and precise bathymetry, utilizing 23 years of satellite altimetry data. Their results indicated that the seabed friction coefficient significantly influences sea level changes in the Persian Gulf. Notably, the tidal behavior in the northern part of Qeshm Island differs from that of other regions in the Persian Gulf. To enhance the accuracy of the hydrodynamic tidal model, the Persian Gulf was divided into two areas, with the seabed friction coefficient modeled separately for each zone.

## 2. Theory of Problem

Some of the notable hydrodynamic flow models include MIKE21, ROMS, HYCOM, COHERENS, and PMODynamics [14], along with FVCOM. The FVCOM model is a open-source Finite-Volume Coastal Ocean Model, originally developed by researchers at Dartmouth University and the Woods Hole Oceanographic Institution. It is widely used by researchers around the world. Initially designed for simulating flooding and drying processes in estuarine dynamical systems, FVCOM has since been upgraded to accommodate a spherical coordinate system, making it suitable for both regional and global applications [15-21].

### 2.1. Governing equations

The governing equations of the FVCOM model in Cartesian coordinates, assuming the absence of snow and ice, include the following components: the equations for momentum, conservation of mass, temperature, salinity, and density, respectively [3]:

$$\begin{aligned} \frac{\partial u}{\partial t} + u \frac{\partial u}{\partial x} + v \frac{\partial u}{\partial y} + w \frac{\partial u}{\partial z} - f v = \\ - \frac{1}{\rho_0} \frac{\partial (P_H + P_a)}{\partial x} - \frac{1}{\rho_0} \frac{\partial q}{\partial x} + \frac{\partial}{\partial z} \left( K_m \frac{\partial u}{\partial z} \right) + F_u \end{aligned} \quad (1)$$

$$\begin{aligned} \frac{\partial v}{\partial t} + u \frac{\partial v}{\partial x} + v \frac{\partial v}{\partial y} + w \frac{\partial v}{\partial z} + f u = \\ - \frac{1}{\rho_0} \frac{\partial (P_H + P_a)}{\partial y} - \frac{1}{\rho_0} \frac{\partial q}{\partial y} + \frac{\partial}{\partial z} \left( K_m \frac{\partial v}{\partial z} \right) + F_v \end{aligned} \quad (2)$$

$$\begin{aligned} \frac{\partial w}{\partial t} + u \frac{\partial w}{\partial x} + v \frac{\partial w}{\partial y} + w \frac{\partial w}{\partial z} = \\ - \frac{1}{\rho_0} \frac{\partial q}{\partial z} + \frac{\partial}{\partial z} \left( K_m \frac{\partial w}{\partial z} \right) + F_w \end{aligned} \quad (3)$$

$$\frac{\partial u}{\partial x} + \frac{\partial v}{\partial y} + \frac{\partial w}{\partial z} = 0 \quad (4)$$

$$\frac{\partial T}{\partial t} + u \frac{\partial T}{\partial x} + v \frac{\partial T}{\partial y} + w \frac{\partial T}{\partial z} = \frac{\partial}{\partial z} \left( K_h \frac{\partial T}{\partial z} \right) + F_T \quad (5)$$

$$\frac{\partial S}{\partial t} + u \frac{\partial S}{\partial x} + v \frac{\partial S}{\partial y} + w \frac{\partial S}{\partial z} = \frac{\partial}{\partial z} \left( K_h \frac{\partial S}{\partial z} \right) + F_S \quad (6)$$

$$\rho = \rho(T, S, P) \quad (7)$$

where the speed components  $x$ ,  $y$ , and  $z$  are respectively the east, north, and vertical axis components in the Cartesian coordinate system. The  $u, v$ , and  $w$  parameters are the  $x, y$ , and  $z$  speed components.  $T, S, \rho, P_a, P_H, q$  respectively indicates temperature, salinity, density, sea-level pressure, hydrostatic pressure, non-hydrostatic pressure, and parameters  $f, g, K_m, K_h$  respectively, express the effect of Coriolis force, gravitational acceleration, the coefficient of vertical eddy viscosity and vertical eddy diffusion of temperature.

Coefficients  $F_u, F_v$  represent horizontal momentum and  $F_T, F_S$  are coefficients of temperature and salinity. Total water depth  $D = H + \zeta$ , where  $H$  is the depth below the water surface (relative to  $z = 0$ ) and  $\zeta$  is the instantaneous water surface height (relative to  $z = 0$ ).  $P = P_a + P_H + q$  is the total pressure at which  $P_H$  the hydrostatic pressure obtained.  $C_d$ , the drag coefficient of a logarithmic lower layer with  $z_{ab}$  of the model is determined at a height higher than the lower layer [3]:

$$C_d = \max \left( k^2 / \ln \left( \frac{z_{ab}}{z_0} \right)^2, 0.0025 \right) \quad (8)$$

where  $k = 0.4$  is Von Karman's constant and  $z_0$  is the bottom roughness parameter.

### 2.2. Sigma coordinate system equations

Due to the variability of water depth across different oceanic regions, particularly near coastal areas and channels, simulating ocean parameters can be challenging. Traditional ocean models utilize a Z-coordinate system in which depth is uniform and rectangular across various areas. However, the influence of water turbulence and mixing in shallow waters cannot be overlooked. Therefore, for more accurate forecasting, it is preferable to use a vertical coordinate system that accounts for different layers with equal distances and fully accommodates the

topography of the seabed. This vertical coordinate system, known as sigma, is employed by the FVCOM hydrodynamic model. In this context,  $\hat{g}=\hat{g}(x,y,r,t)$  represents a generalized Earth coordinate system where  $x$  and  $y$  denote the east and north axes, respectively, and  $r$  is the vertical axis, ranging from -1 to 0. The variable  $r$  can be defined as a sigma, composite, or more generalized function [22].

The hydrodynamic model employs  $s$ -coordinates in deep water and  $\sigma$ -coordinates in shallow water to resolve the equations. Since the Khuran channel is located in a shallow water region, the model utilizes the  $\sigma$ -coordinate system.

### 2.3. Time step determination

The sea level height describes fast-moving long surface gravity waves. In the explicit numerical method, the time step selection criterion is inversely proportional to the phase speed of the waves, represented as  $(\sqrt{gd})$ .

Since the sea level height is proportional to the water transport gradient, it can be calculated using vertically integrated equations. Subsequently, the three-dimensional equations can be solved with a specified sea level height. In this numerical method, known as "mode splitting," the currents are divided into external and internal currents, which can be calculated using two separate time steps. This method is also successfully implemented in models such as POM1 and ROMS2.

## 3. Experimental investigations

### 3.1. Input data

There are two common current measurement methods including Eulerian and Lagrangian approaches. The point Acoustic Current Meter, RCM9, employs the Eulerian method for current measurement. One of the input data sets for the FVCOM hydrodynamic model is the bathymetric data obtained from hydrographic operations in the Khuran Strait. These bathymetric data, collected using a single beam echo sounder, were gridded using Surface Water Modelling System (SMS) software. As an integrated grid on the horizontal surface of the fluid, tidal components at open border points on both sides of the Khuran channel were extracted as a time series using the Tidal Model Driver (TMD) tidal model. This extraction ensured that the required inputs could be formatted according to the specifications in the FVCOM user manual. Additional data, such as depth, salinity, density, and temperature, were also introduced to the model, considering the physics of the sea. The program was then run in a Linux environment. Finally, using MATLAB and other software, we processed the resulting data from the output file and compared and analyzed it with direct observations

obtained from the RCM9 current meter installed near Shahid Rajae Port.

### 3.2. Mesh grid

The SMS software, within the Aqua module, was used to produce bathymetry gridding taken in the Quran Strait. Following the standards of the International Hydrographic Organization (IHO), these measurements were conducted using a single-beam system to create bathymetric charts. Node spacing was designated based on proximity to the coastline as follows: 100 meters near coastlines, 200 meters in central grid points, and 400 meters in distant regions. The model's bathymetry is illustrated in Figure 2. A large grid comprising 50,161 node points fully covered the study area, with region-specific spacing for enhanced accuracy. A finer mesh was applied along closed (dry) boundaries where the coastline's shape and complexity increased, whereas larger cells in central regions were used to enhance grid conformity to the coastline. Coastal boundary points were derived from field surveys (as shown in Figure 3).

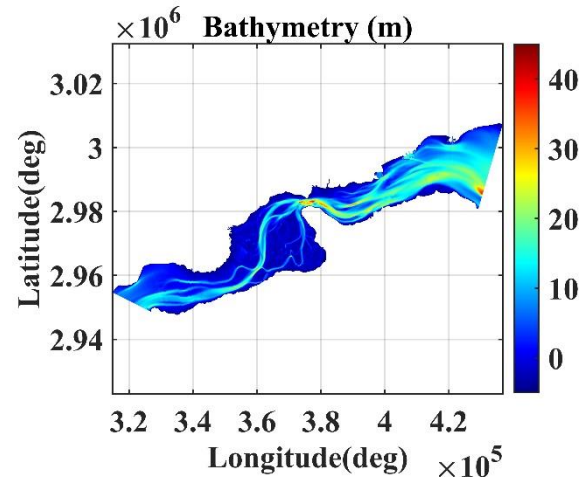


Figure 2. Bathymetric map of the Khuran Channel

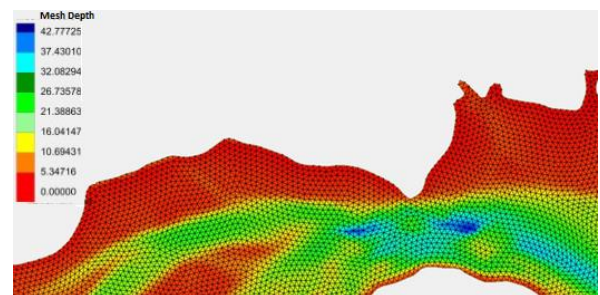


Figure 3. Mesh grid of case study derived by FVCOM model

### 3.3. Boundary conditions, open and closed boundaries

The Khuran channel, situated between Qeshm Island to the south and the mainland coastline to the north, was represented in the model with closed land boundaries on the northern and southern sides and open boundaries on the eastern and western sides. The TMD, a MATLAB code, was utilized to access

<sup>1</sup> Princeton Ocean Model

<sup>2</sup>Regional Ocean Modelling System

harmonic tidal model components essential for predicting tidal heights and currents. The model incorporated eight tidal components ( $M_2$ ,  $S_2$ ,  $K_2$ ,  $N_2$ ,  $K_1$ ,  $P_1$ ,  $O_1$ , and  $Q_2$ ) based on latitude and longitude coordinates.

To run the FVCOM program, 85 open boundary points were introduced, and tidal time series data generated from TMD tidal model components were processed in parallel on a Linux environment. The output file, saved in NetCDF (NC) format, was subsequently analyzed using MATLAB to extract parameters such as instantaneous water level height, amplitude, phase, current speed, and direction. These values were computed across 98,282 elements and 50,161 nodes at seven sigma levels, with a focus on the middle layer of the third sigma level. Data outputs—documented in Julian day, UTC local time, speed (in meters per second), and direction (in degrees)—were obtained from the FVCOM hydrodynamic model. The accuracy of this data was validated against observations from Shahid Rajaei station using statistical methods including Root Mean Square Error (RMSE), Q-Q plots, and scatter plots.

For sensitivity calibration, the model was initially run with varying roughness values, eventually identifying an optimal roughness value of 0.0066 based on a comparison of estimated results. Calibration was conducted at a temperature of 23°C and a salinity of 36.5, with calculations performed in 10-minute time steps. The model used a sigma coordinate system to divide the water column into seven levels, with a middle layer flanked by three levels above and three levels below, thus forming a 7-sigma level structure.

Tidal currents in this model are influenced by factors such as temperature, salinity, wind, seabed topography, and water depth, resulting in complex and dynamic coastal water movement patterns. These factors significantly impact coastal climate, sediment transport, organic and chemical substance distribution, environmental health, marine transportation, fisheries, marine energy generation, coastal structures, and infrastructure, including oil installations and pipelines. Tidal component data were integrated into the model as a continuous time series applied to open boundary points on both the eastern and western sides of the study area, spanning from the Bandar Abbas old port to the Bahman port in the east, and from Hameyran to Basaidu in the west. Tidal current observations at the Shahid Rajaei and Pohl stations include three main data columns: time, current speed, and direction, with a sampling rate of 10 minutes. These datasets, prepared by Darya Tarsim Consulting Engineers Company, were collected at a sampling rate of ten minutes over a three-month period as shown in Table 1.

Shahid Rajaei	27.11	56.06	3 months	2009	10
Pohl	26.96	55.37	3 months	2009-2010	10

The model’s simulated results were then compared with direct measurements from the Shahid Rajaei and Pohl stations, and the findings are summarized as follows.

**3.4. Sensitivity analysis**

Accurate calibration of the hydrodynamic model requires an effective bed roughness parameter, as bed roughness introduces friction that affects bed shear stress, resulting in resistance and delay in current flow. This parameter is quantified by the drag coefficient, which impacts the amplitude and phase of the tidal model’s harmonic components. In the Khuran area, no direct measurements of bed roughness have been conducted to date.

Bed roughness represents resistance to flow and includes the shear stress exerted by the seabed. This parameter depends on the seabed’s relief and particle size (e.g., sand, clay, and sediments). Although the seabed is dynamic, bed roughness is assumed to remain constant over time, as average changes in seabed shape are considered stable.

To assess model sensitivity, we ran the hydrodynamic model with Manning values of 0.0037, 0.0044, 0.0066, and 0.0088 over three-day intervals from October to January, a period capturing the highest variability. A Manning value of 0.0066 was identified as the optimal bed roughness coefficient, as it minimized the difference between model outputs and tidal observations.

**3.5. Statistical reliability and model validity**

The model’s accuracy is assessed by comparing its results with those from other studies, using statistical methods to evaluate reliability and validity while accounting for variance. Statistical metrics, including Root Mean Square Error (RMSE), Relative Variance (RV), and the Coefficient of Determination ( $R^2$ ), are applied to evaluate the model’s performance, as defined by the following mathematical equations.

The RMSE equation is as follow:

$$RMSE = \sqrt{\frac{[h_t - h(t)]^2}{N}} \tag{9}$$

In the RMSE equation,  $h(t)$  is the predicted value and  $h_t$  is observed values and  $N$  is the number of observations. The closer the answer is to zero, the better the accuracy of the model.

RV is the reduction of variance that expresses the ratio of the variance of the predicted values to the variance of the observed values according to the following equation:

**Table 1. Stations of tidal current observation**

Station	$\phi$	$\lambda$	period of observation	year	Sample rate (minutes)
---------	--------	-----------	-----------------------	------	-----------------------

$$RV = \frac{\sum [h(t) - h_0]^2}{\sum [h_t - h_0]^2} \quad (10)$$

where  $h_0$  is the average value of observations and  $h_t$  is the value of observation, and  $h(t)$  is the predicted values. If  $RV$  is equal to one, it indicates the agreement of observations and predictions. The Coefficient of Determination (R-squared or  $R^2$ ) is as follow:

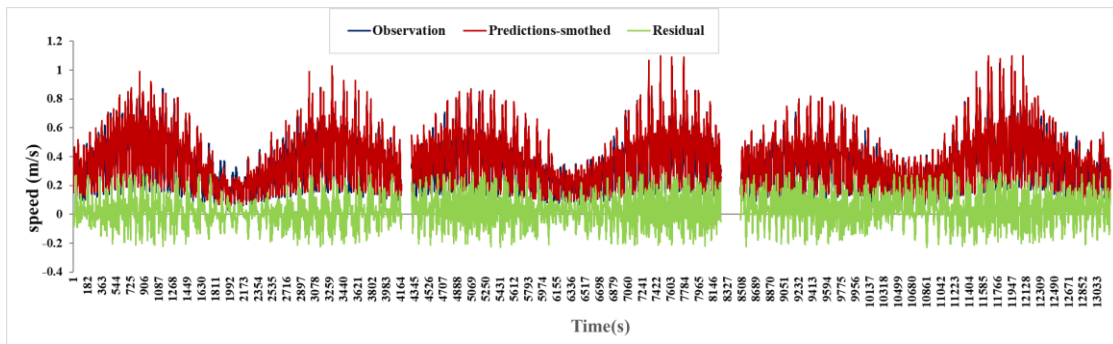
$$R^2 = 1 - \frac{\sum (h_t - h(t))^2}{\sum (h_t - h_0)^2} \quad (11)$$

### 3.6. Current speed

The statistical evaluation of the FVCOM hydrodynamic model for current speed at the Port of Shahid Rajae showed strong agreement between observed and predicted values. The Root Mean Square Error (RMSE) was 0.095 m/s, and the Relative

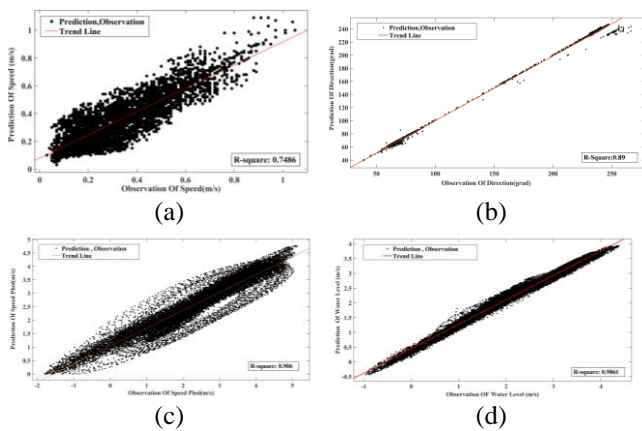
Variance (RV) was 1.078, indicating high accuracy. Moreover, the Coefficient of Determination ( $R^2$ ) of 0.756 confirmed a strong correlation between model results and observations, further validating the model's reliability in predicting tidal current speed. If the bed roughness parameter had not been optimized and calibrated, the model could have overestimated or underestimated flow velocities. However, as expected, this did not occur in our modeling study.

Figure 4 presents a comparison between observed current speed data and FVCOM hydrodynamic model results, sampled at 10-minute intervals. A moving average filter was applied to the observed data to reduce random noise. The strong agreement between the simulated and observed data, as shown in the figure, demonstrates the ability of the model to simulate the flow velocity.



**Figure 4. Comparison of the speed values of the measured observations with the results obtained of the model**

Tidal flow simulations were conducted for Shahid Rajae station, where current meter observations were collected at 10-minute intervals over a three-month period, encompassing both low and high tide cycles. For a more detailed analysis, Figures 5a and 5b show a scatter plot comparing observed and predicted current speed and direction at the station.



**Figure 5. Scatter plots: (a) comparison of predicted and observed speeds in Rajae port (b) predicted vs observed for current directions in Rajae port (c) comparison of predicted and observed of current speeds in Pohl port (d) water level of Shahid Rajae port observed vs. predicted**

The data presented indicates that the observations and predictions from the FVCOM model at Shahid Rajae port station demonstrate a strong correlation between model data and actual observations, with negligible residual values.

The Q-Q plot in Figure 6a indicates a good agreement between the model-predicted and observed data, with a high density of points along the diagonal line. While there are some deviations in the initial and final values, these discrepancies are relatively small compared to the overall dataset.

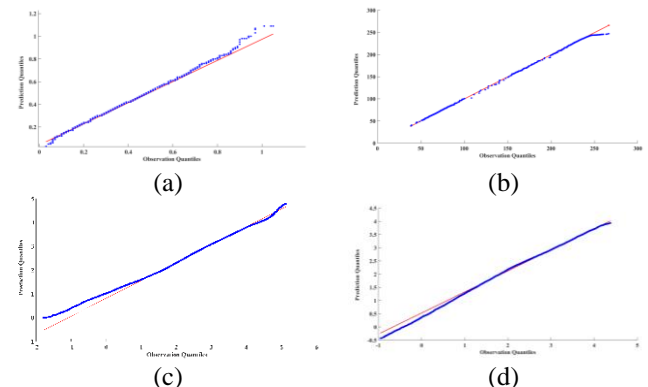


**Figure 6. Q-Q plots: (a) for comparison of predicted and observed speeds in Rajae port, (b) comparison of predicted and observed directions in Rajae port, (c)**

**comparison of predicted and observed current speeds in Pohl port, (d) water level of Shahid Rajae port observed vs. predicted**

**3.7. Current direction**

The model-predicted flow directions, expressed in degrees, align well with the observed directions at Shahid Rajae station. The relatively low values of Relative Variance (RV = 1.02) and Root Mean Square Error (RMSE = 0.8417 m/s) indicate a strong

correlation between observed and predicted speed values, with a correlation coefficient of 89%. Instances of rapid changes in direction, which can lead to high-angle rotations, were excluded from the analysis. The statistical metrics and visual comparisons (Figure 7) demonstrate excellent agreement between the model-predicted and observed directions at Shahid Rajae port.

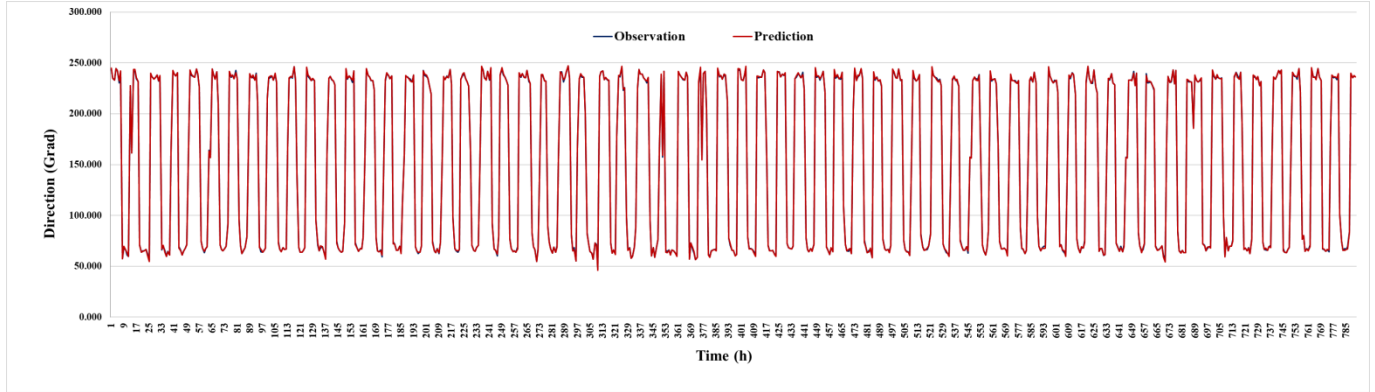


**Figure 7. Agreement of the observations of the predicted and observed directions**

**3.8. Water level**

Using the output of the information obtained from the FVCOM hydrodynamic model, the water level has been shown in Figure 8.

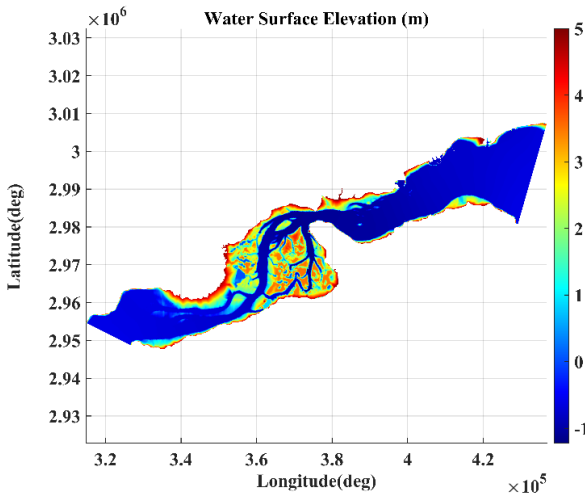


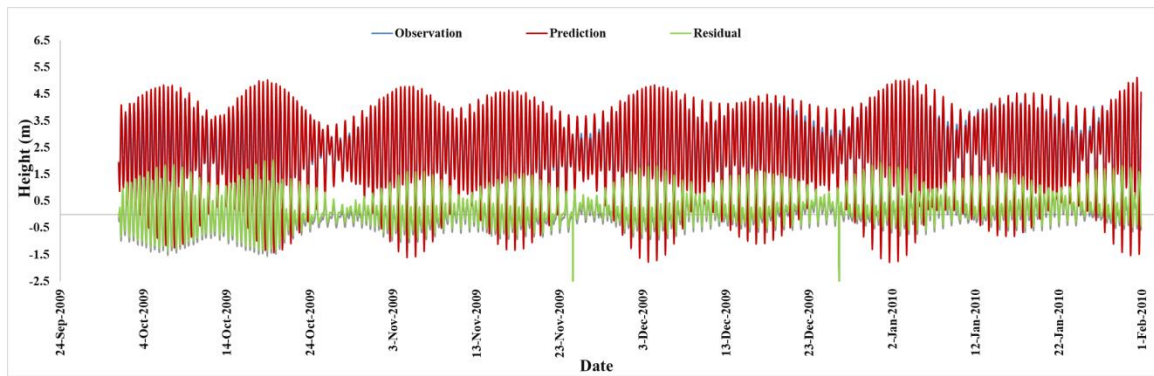
**Figure 8. Water level plot in the Khuran Channel area**

The model simulations were conducted using a roughness coefficient of 0.0066 and a vertical discretization of 7 sigma levels. To further validate the model's performance, additional simulations were carried out for the Port of Pohl station.

Comparisons of simulated and observed water levels at both the Port of Pohl and Shahid Rajae stations demonstrate excellent agreement (Figures 9a and 9b). The statistical results of this modelling for water level prediction are shown in the table 2. below.

**Table 2. Comparison of the values of the analysis accuracy indices**

Station	RMSE (m/s)	RV	R <sup>2</sup>	Sample rate(minutes)
Shahid Rajae	0.22	1.22	0.89	10
pohl	0.58	1.11	0.75	10



(a)

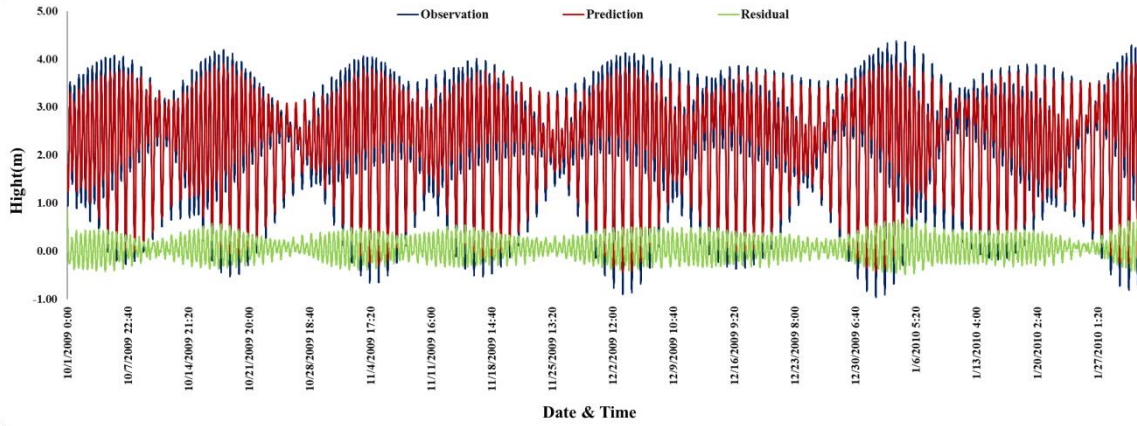


**Figure 9. Comparison of height observations the water level: (a) in Port of Pohl vs the model results, (b) in Port of Shahid Rajae vs model results**

**3.9. Tidal Current Diamond**

One of the goals of simulating the speed and flow in Khuran is to produce a tidal current diamond tables that can be inserted in nautical charts. Tidal Current Diamonds are symbols on British and international nautical charts that indicate the direction and speed of tidal currents relative to High Water times as specified in the Admiralty Tide Tables.

These tables are typically found on nautical charts and consist of a grid with 13 rows and 3 columns for each diamond. The first column indicates the time relative to High Water, ranging from 6 hours before to 6 hours after. The remaining columns provide the mean direction and speed of tidal currents during spring and neap tides at specific locations. While Tidal Current Diamonds provide valuable information, Tidal Atlases, when available, often offer more accurate and user-friendly representations of tidal currents.

Table 3 compares the values of the speeds and directions of the simulated tidal current with the values published in the Iranian navigation chart of Khuran region.

**4. Conclusions**

FVCOM hydrodynamic model was utilized in the Khuran Channel of the Persian Gulf to simulate tidal currents and water levels. The model's performance was evaluated by comparing simulated and observed data for current speed, direction, and water level.

The results indicate a strong agreement between simulated and observed values. The model accurately captured the spatial and temporal variability of tidal currents, with a Root Mean Square Error (RMSE) of 0.095 m/s for current speed and a high correlation coefficient ( $R^2$ ) between observed and predicted values.

The Q-Q plots further confirmed the good agreement between simulated and observed distributions.

The sensitivity analysis revealed that the model's performance is influenced by the bed roughness coefficient. However, with appropriate calibration, the model can provide reliable predictions. Overall, the

FVCOM hydrodynamic model demonstrated its ability to accurately simulate tidal hydrodynamics in the study area, providing valuable insights for coastal engineering and environmental management.

**Table 3. Tidal Current Diamond around Shahid Rajae port**

TIDAL STREEM	DIR.(DEG.)	RATE (KNOT)		DIR.(DEG.)		
		SPRING	NEAP	SPRING	NEAP	
6hours before H.W	75	0.7	0.3	60	0.4	0.2
5hours before H.W	45	0.3	0.1	29	0.6	0.3
4hours before H.W	300	0.5	0.2	304	0.6	0.5
3hours before H.W	263	1.0	0.5	265	1.0	0.6
2hours before H.W	250	1.5	0.7	257	1.4	0.4
1hours before H.W	246	1.2	0.6	249	1.1	0.2
H.W	247	0.7	0.3	247	0.7	0.3
1hours after H.W	342	0.2	0.1	243	0.5	0.4
2hours after H.W	65	0.3	0.1	231	0.7	0.5
3hours after H.W	89	0.7	0.3	75	0.7	0.5
4hours after H.W	70	1.1	0.5	60	1.2	0.5
5hours after H.W	79	1.3	0.6	60	1.1	0.4
6hours after H.W	76	1.0	0.5	67	0.7	0.3

From the results of the model, we were able to extract a prediction of the necessary tidal current speeds and directions in the form of a Tidal Current Diamond for inclusion in navigational charts.

**Acknowledgment**

The authors are thankful to Geospatial-based Hydrologic Laboratory (School of Surveying and Geospatial Engineering, College of Engineering, University of Tehran) for supporting this research.

## 8. References

1. Foreman, M.G.G., *Manual for tidal heights analysis and prediction*. 1977: Institute of Ocean Sciences, Patricia Bay.
2. ZANGANEH, A.M., M.E. TAGHAVI, and E. AKBARI, *Evaluation and assessment of changes in forest area Harra (mangrove) Using remote sensing techniques Case Study: Bandar Abbas*. 2017.
3. Chen, C., H. Liu, and R.C. Beardsley, *An unstructured grid, finite-volume, three-dimensional, primitive equations ocean model: application to coastal ocean and estuaries*. Journal of atmospheric and oceanic technology, 2003. **20**(1): p. 159-186.
4. Wu, X.-g. and H.-s. Tang, *Coupling of CFD model and FVCOM to predict small-scale coastal flows*. Journal of Hydrodynamics, Ser. B, 2010. **22**(5): p. 284-289.
5. Cowles, G.W., *Parallelization of the FVCOM coastal ocean model*. The International Journal of High Performance Computing Applications, 2008. **22**(2): p. 177-193.
6. Sabatino, A.D. and I. Thurlbeck, *FVCOM Clyde Sea Hydrodynamic Model User Guide and Technical Report*. 2016.
7. Li, S. and C. Chen, *Air-sea interaction processes during hurricane Sandy: Coupled WRF-FVCOM model simulations*. Progress in Oceanography, 2022. **206**: p. 102855.
8. Xu, H., M. Canals, and A. Rivera. *High Resolution Modeling of Coastal Circulation Using FVCOM in Puerto Rico and the US Virgin Islands*. in *OCEANS 2022-Chennai*. 2022. IEEE.
9. Bairamzadeh, M., S.M. Siadat Mousavi, and M. Majidi, *Modeling the current pattern of Persian Gulf and Sea of Oman using FVCOM model*, in *16 th Iranian Hydraulics Conference papers*. 2018: Ardabil, Iran.
10. Razzaghi, S., et al., *3D Numerical Modelling of Shallow and Deep Water Currents in the Persian Gulf*. Iranian Journal of Geophysics, 2019. **13**(3): p. 69-85.
11. Sadrinasab, M., et al., *Numerical Modelling of Arvandrud River Plume and the impact of wind and River Discharge on the plume structure By Three Dimensional and Hydro dynamical Model (FVCOM)*. Journal of Marine Science and Technology, 2021. **20**(3): p. 12-30.
12. Shariatmadari, D., M. Siadat-Mousavi, and C. Ershadi, *Evaluation of extractable energy from tidal farm in the Qeshm canal using numerical flow simulation*. Journal of Oceanography, 2021. **12**(46): p. 1-12.
13. Sohrabi Athar, M., A.A. Ardalan, and R. Karimi, *Hydrodynamic tidal model of the Persian Gulf based on spatially variable bed friction coefficient*. Marine Geodesy, 2019. **42**(1): p. 25-45.
14. Bakhtiari, A., et al., *An Investigation on PMO Dynamic Model in Bushehr Bay, Persian Gulf, Iran*. Journal of Oceanography, 2013. **4**(14): p. 13-18.
15. Chen, C., R. Beardsley, and G. Cowles, *An unstructured grid, finite-volume coastal ocean model (FVCOM) system*. Oceanography, 2006. **19**(1): p. 78-89.
16. Darya Tarsim Company, D.B.T.F. 2023.
17. DHI, *MIKE 21 Toolbox - Global Tide Model – Tidal prediction*.
18. Fossette, S., et al., *A biologist's guide to assessing ocean currents: a review*. Marine Ecology Progress Series, 2012. **457**: p. 285-301.
19. John, B., et al., *COHERENS: a hydrodynamic model validated for the west coast of India*. Current Science, 2015: p. 288-300.
20. Lyard, F.H., et al., *FES2014 global ocean tide atlas: design and performance*. Ocean Science, 2021. **17**(3): p. 615-649.
21. Shchepetkin, A.F. and J.C. McWilliams, *The regional oceanic modeling system (ROMS): a split-explicit, free-surface, topography-following-coordinate oceanic model*. Ocean modelling, 2005. **9**(4): p. 347-404.
22. Chen, C., et al., *An unstructured-grid, finite-volume community ocean model: FVCOM user manual*. 2012: Sea Grant College Program, Massachusetts Institute of Technology Cambridge ....